

CR 61583

SIMULATED LOW-GRAVITY SLOSHING IN SPHERICAL TANKS AND CYLINDRICAL TANKS WITH INVERTED ELLIPSOIDAL BOTTOMS

by

Frank T. Dodge

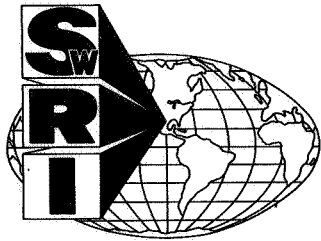
Luis R. Garza

Technical Report No. 6
Contract NAS8-20290
Control No. DCN 1-6-75-00010
SwRI Project No. 02-1846

Prepared for

George C. Marshall Space Flight Center
National Aeronautics and Space Administration
Huntsville, Alabama

February 1968



SOUTHWEST RESEARCH INSTITUTE
SAN ANTONIO



ERRATA--19 February 1968

The following corrections should be made to Technical Report No. 5, Contract NAS8-20290, entitled "Simulated Low Gravity Sloshing in Cylindrical Tanks Including Effects of Damping and Small Liquid Depth." All the corrections arise from a labeling error in Figure 11 of the report.

1. Page 8, 2nd line above Eq. (8). The value of A should be 8.20 instead of 0.63 as given; the value of n should be -3/5 instead of -1/2 as given.
2. Page 9, line 2. The value of N_{BO} should be 4.0 instead of 0.03 as given.
3. Page 9, lines 5 and 6. Delete the lines given and replace by "...of Ref. [7], but, for $N_{BO} = 4.0$, Eq. (2) predicts that $\gamma_s = 0.83 N_{GA}^{-1/2} + 0.042$, which is about of the correct numerical magnitude. Note, also, that γ_s varies with N_{BO} in the same way in both Eq. (2) and Eq. (8)."
4. Page 12, 2nd equation after line 6. This equation should read, " $\gamma_s = 0.83 N_{GA}^{-1/2} (1 + 8.20 N_{BO}^{-3/5})$," instead of as given.
5. Page 27, Figure 11. The equation given on the figure should read,
$$\frac{\gamma_s - 0.83 N_{GA}^{-1/2}}{0.83 N_{GA}^{-1/2}} = 8.20 N_{BO}^{-3/5}.$$

SOUTHWEST RESEARCH INSTITUTE
8500 Culebra Road, San Antonio, Texas 78228

Department of Mechanical Sciences

**SIMULATED LOW-GRAVITY SLOSHING IN
SPHERICAL TANKS AND CYLINDRICAL TANKS
WITH INVERTED ELLIPSOIDAL BOTTOMS**

by

Frank T. Dodge

Luis R. Garza

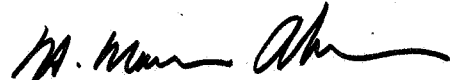
**Technical Report No. 6
Contract NAS8-20290
Control No. DCN 1-6-75-00010
SwRI Project No. 02-1846**

Prepared for

**George C. Marshall Space Flight Center
National Aeronautics and Space Administration
Huntsville, Alabama**

February 1968

Approved:



**H. Norman Abramson, Director
Department of Mechanical Sciences**

FOREWORD

This report is the fourth in a series of Technical Reports concerned with fuel sloshing under low-gravity conditions. Reference to the first three reports ("Experimental and Theoretical Studies of Liquid Sloshing at Simulated Low Gravities," TR No. 2, Contract NAS8-20290, 20 October 1966; "Low Gravity Liquid Sloshing in an Arbitrary Axisymmetric Tank Performing Translational Oscillations," TR No. 4, Contract NAS8-20290, 20 March 1967; and "Simulated Low-Gravity Sloshing in Cylindrical Tanks Including Effects of Damping and Small Liquid Depth," TR No. 5, 29 December 1967) will aid in understanding some of the experimental procedures and theoretical analyses that are presented in abbreviated form in the present report.

ABSTRACT

Liquid sloshing in cylindrical tanks having inverted ellipsoidal bottoms and in spherical tanks is studied experimentally under conditions of simulated low gravities. The effects of variable liquid depth and the determination of the smooth wall damping are emphasized. Results from cylindrical tanks are qualitatively similar to results obtained previously with cylindrical tanks having flat bottoms; significant differences from previous results for natural frequency and slosh damping are apparent, however, for small liquid depths. Correlation equations for the damping coefficient as a function of h/d , N_{GA} , and N_{BO} are presented. Results from spherical tanks show that the variation in free surface curvature with liquid depth has a strong effect on the natural frequency; in fact, increased curvature in spherical tanks as compared to cylindrical tanks causes the natural frequency to decrease as N_{BO} decreases, which is just the opposite of the variation obtained with cylindrical tanks. The damping in spherical tanks is shown to be a minimum when the tank is half-full; when $h_{av}/d = 0.50$ (half-full), γ_s is about 50% less than γ_s when $h_{av}/d = 0.25$, and about 10 to 20% less than when $h_{av}/d = 0.75$.

TABLE OF CONTENTS

	<u>Page</u>
LIST OF ILLUSTRATIONS	v
LIST OF TABLES	vi
I. INTRODUCTION	1
II. EXPERIMENTAL APPARATUS AND PROCEDURES	2
III. RESULTS FOR CYLINDRICAL TANKS WITH INVERTED ELLIPSOIDAL BOTTOMS	3
A. Force Response	3
B. Natural Frequency	4
C. Slosh Damping	4
IV. RESULTS FOR SPHERICAL TANKS	8
A. Force Response	9
B. Natural Frequency	10
C. Slosh Damping	11
V. CONCLUSIONS	15
LIST OF REFERENCES	16
APPENDIX -- ILLUSTRATIONS	17

LIST OF ILLUSTRATIONS

<u>Figure</u>		<u>Page</u>
1	Tanks and Dynamometer Used in Tests	18
2	Force Response Curves for Methanol in 1.36-In. Cylindrical Tank, $N_{BO} = 100$	19
3	Force Response Curves for Methanol in 1.04-In. Cylindrical Tank, $N_{BO} = 60$	20
4	Force Response Curves for CCl_4 in 0.688-In. Cylindrical Tank, $N_{BO} = 45$	21
5	Force Response Curves for Methanol in 0.688-In. Cylindrical Tank, $N_{BO} = 26$	22
6	Force Response Curves for CCl_4 in 0.383-In. Cylindrical Tank, $N_{BO} = 14$	23
7	Variation of Natural Frequency Parameter in Cylindrical Tanks with Bond Number	24
8	Variation of Damping Coefficient with Galileo Number, $h/d = 1.25$	25
9	Damping Coefficient Versus $0.83 N_{GA}^{-1/2} (1 + 8.20 N_{BO}^{-3/5})$, $h/d = 1.25$	26
10	Damping Coefficient Versus $1.23 N_{GA}^{-1/2} (1 + 2.20 N_{BO}^{-3/5})$, $h/d = 0.50$	27
11	Damping Coefficient Versus $1.65 N_{GA}^{-1/2} (1 + 1.22 N_{BO}^{-3/5})$, $h/d = 0.25$	28
12	Force Response Curves for CCl_4 in 1.36-In. Spherical Tank	29
13	Force Response Curves for Methanol in 1.36-In. Spherical Tank	30
14	Force Response Curves for Acetone in 1.36-In. Spherical Tank	31
15	Force Response Curves for Methanol in 1.04-In. Spherical Tank	32

LIST OF ILLUSTRATIONS (Cont'd)

<u>Figure</u>		<u>Page</u>
16	Force Response Curves for Acetone in 1.04-In. Spherical Tank	33
17	Variation of Natural Frequency Parameter in Spherical Tanks with Bond Number	34

LIST OF TABLES

<u>Table</u>		<u>Page</u>
I	Summary of Damping and Frequency Data Cylindrical Tanks with Inverted Ellipsoidal Bottoms	5
II	Diameter of Free Surface and Percentage Fullness of Tank	8
III	Summary of Damping and Frequency Data Spherical Tanks	12

I. INTRODUCTION

It is now well recognized that the behavior of contained liquid fuels under reduced gravity conditions is as important to the success of a space system's mission as the behavior of the liquid under normal gravity or thrusting conditions. Unfortunately, the lack of an easily accessible low-gravity laboratory has prevented the gathering of engineering data under truly low-gravity conditions; but, for some purposes, such as determining the slosh behavior of the liquid fuel, it is acceptable to simulate low-g (i.e., small Bond numbers) by using tanks of such small diameter in the tests that the forces at the liquid-free surface are comparable to the body or gravity forces. Valuable data on slosh forces, frequencies, and damping have already been obtained by this method [1, 2, 3, 4].† Furthermore, in those cases where theoretical results or actual low-g data exist, the results obtained using simulated low-g compare very well to them.

The purpose of the work reported here was to conduct an exploratory program of research concerned with sloshing under moderately low simulated gravities (Bond numbers of about 10 to 100) in two different tank geometries of practical interest, namely, spherical tanks and cylindrical tanks with inverted ellipsoidal bottoms. Three different liquids (carbon tetrachloride, methanol, and acetone) were tested in two different spherical tanks (diameters: 1.36 in. and 1.04 in.) and four different cylindrical tanks (diameters: 1.36 in., 1.04 in., 0.688 in., and 0.383 in.). The cylindrical tanks were made of glass, although the bottoms were aluminum, but, for fabrication reasons, the spherical tanks were made entirely of aluminum. The ellipsoidal bottoms of the cylindrical tanks were all geometrically similar and had ratios of major to minor diameters (base to height) of $\sqrt{2}$ to 1.

†Numbers in brackets denote references listed in Section VI of this report.

II. EXPERIMENTAL APPARATUS AND PROCEDURES

The experimental setup used in the present tests was similar to that described in Ref. [4]. A photograph of the four cylindrical tanks and two spherical tanks used in the tests is shown in the top half of Figure 1, and a view of a cylindrical tank and a spherical tank in the dynamometer package (with its protective cover) is shown in the bottom half of the figure; in the actual experiments, of course, only one kind of tank is used in any one test.

Experimental procedures, calibrations, and data reductions were the same as reported previously [2]. Briefly, however, two tanks were used for each test; one tank, empty and called the balance tank, was used to cancel the inertia of the other tank, containing the test liquid and called the active tank, so that the residual force felt by the dynamometer when the active tank was empty was very small. The sloshing force was detected by semiconductor strain gages (gage factor = 118) mounted on the tension-compression arms of the dynamometer; the output of the gages was amplified, filtered, and recorded on an oscilloscope. The excitation frequency, which could be maintained to the fourth significant figure of the period (in seconds), was determined with a digital period counter.

III. RESULTS FOR CYLINDRICAL TANKS WITH INVERTED ELLIPSOIDAL BOTTOMS

There were two main objectives of this part of the experimental program: (1) measure the lateral slosh force for the fundamental mode as a function of the excitation frequency and amplitude, and (2) measure the slosh damping in the bare-wall tanks. The parameters to be varied were the Bond number and the liquid depth.

All the tests were run with glass tanks having aluminum bottoms and reagent grade liquids. As nearly as could be determined visually, the contact angle of all the liquids on the glass walls was zero degrees, and the slosh wave appeared to approximate very well the "free edge" or no contact angle hysteresis condition.

A. Force Response

Figures 2 through 6 show typical force response curves for CCl_4 and methanol. (The force response of acetone is not shown since in every case it was nearly identical to that of methanol.) The solid lines in the figures are faired curves through the experimental data. Because, in the absence of a low- g theory for tanks of this geometry, no meaningful method of nondimensionalizing the slosh forces is known, the curves are given in dimensional terms; this should facilitate direct comparisons when a theory does become available. Note that the combination of small excitation amplitudes, very little out-of-plane motion of the shake table, and the natural slosh damping allowed complete resonance curves to be obtained; that is, no liquid swirling at resonance was evident.

The range of Bond numbers, $N_{BO} = \rho g R_o^2 / T$, covered in the figures is 100 (methanol in 1.36-in. diameter tank) to 14 (CCl_4 in 0.383-in. diameter tank). Except in Figure 6, the values of h/d shown in the figures are always the same; 1.25, 0.50, and 0.25.[†] In Figure 6, corresponding to a tank diameter of 0.383 in. and $N_{BO} = 14$, the mass of liquid in the tank for $h/d = 0.25$ was so small that the output force signal was not large enough to give good readings on the oscilloscope; thus, $h/d = 0.375$ was substituted here. It is felt that further improvements in the dynamometer and recording system will overcome this handicap. Other data given in the figures include the amplitude of tank excitation (x_o , inches), the resonant frequency (f_1 , cps) determined by the peak in the response curve, the slosh damping coefficient (γ_s) determined by the half-bandwidth technique, and the wave height (δ , inches) at resonance.

[†] h is the depth of liquid from the bottom of the curved meniscus to the top of the inverted ellipsoidal bottom. The average liquid depth is larger than h by an amount equal to $(\sqrt{2/12} + 0.132\beta)d$ where β is the root of $\beta^3 N_{BO} - \beta^2 - 2/3 = 0$.

The response curves are reasonably linear (that is, doubling x_0 doubles the forces) except that they are slightly "softening" inasmuch as f_1 decreases with increased x_0 ; also, γ_s depends slightly on x_0 .

B. Natural Frequency

The excitation frequency at which the maximum force occurs can be determined from the response curves. This "resonant" frequency differs from the "natural" frequency by an amount which depends on the damping. Assuming that a suitable equivalent mechanical model is a mass-spring-dashpot system, a model known to be correct for a wide variety of sloshing motions, the resonant frequency and the natural frequency are related through the equation

$$f_1 = f_1^*(1 - 2\gamma_s^2)^{1/2} \quad (1)$$

in which f_1 is the resonant frequency, f_1^* the natural frequency, and γ_s the damping coefficient. The nondimensional natural frequency parameter $(2\pi f_1^*)^2 R_o/g$ computed using Eq. (1) is shown for all the tests in the last column of Table I on the next page. As can be seen, the difference between $(2\pi f_1)^2 R_o/g$ and $(2\pi f_1^*)^2 R_o/g$ is small for the large tanks but noticeable for the smaller tanks.

The frequency parameter, $(2\pi f_1^*)^2 R_o/g$, as a function of Bond number and h/d is also shown graphically in Figure 7, in which the solid curves are faired through the data. Because f_1^* decreases with increasing x_0 , the frequencies plotted on the graph are always for the smallest value of x_0 , whenever a choice existed. For comparison purposes, values of $(2\pi f_1^*)^2 R_o/g$ for $N_{BO} = \infty$ and flat bottom tanks are also shown on the figure.

The experimental natural frequency generally increases as the Bond number decreases, although the increase is not so great as occurs in flat bottom tanks [2, 4]. In fact, at $h/d = 1.25$, for which the liquid depth is large enough that one would expect no differences between flat and inverted ellipsoidal bottoms, the experimental frequency is larger than the flat bottom $N_{BO} = \infty$ limit only for $N_{BO} < 14$; in flat bottom tanks [4], however, the frequency equals this $N_{BO} = \infty$ limit at about $N_{BO} = 40$ and is about 8% larger at $N_{BO} = 14$. It is difficult to rationalize the reasons for this discrepancy between the two results.

C. Slosh Damping

The slosh damping coefficient was determined by the half-bandwidth technique for all the tests, with the results shown in Table I. The damping coefficient, γ_s , for $h/d = 1.25$ is also shown graphically on Figure 8 as a function of the Galileo number, $N_{GA} = \nu^{-1} R_o^{3/2} g^{1/2}$; for comparison

TABLE I. SUMMARY OF DAMPING AND FREQUENCY DATA CYLINDRICAL
TANKS WITH INVERTED ELLIPSOIDAL BOTTOMS

Tank Diameter (in.)	Liquid	N_{BO}	$N_{GA}^{-1/2}$	h/d	x_o (in.)	γ_s	f_1 (cps)	$(2\pi f_1)^2 \frac{R_o}{g}$	$(2\pi f_1^*)^2 \frac{R_o}{g}$
1.36	CCl_4	1.75	0.0089	1.250	0.0015	0.011	5.08	1.795	1.795
				0.500	0.002	0.012	4.99	1.732	1.732
				0.250	0.002	0.015	4.65	1.504	1.504
1.36	Methanol	1.00	0.0099	1.250	0.002	0.013	5.07	1.788	1.788
				0.500	0.002	0.014	5.00	1.739	1.739
				0.250	0.002	0.016	4.65	1.504	1.504
1.04	Methanol	60	0.0121	1.250	0.002	0.017	5.78	1.777	1.777
				0.500	0.002	0.017	5.72	1.741	1.741
				0.250	0.003	0.020	5.64	1.692	1.693
0.688	CCl_4	45	0.0149	1.250	0.002	0.020	7.12	1.784	1.785
				0.500	0.002	0.022	7.07	1.729	1.731
				0.250	0.002	0.021	6.93	1.759	1.761
0.688	CCl_4	45	0.0149	0.500	0.002	0.022	6.64	1.552	1.553
				0.250	0.003	0.024	6.56	1.514	1.516
				0.125	0.003	0.025	6.50	1.516	1.516

TABLE I. SUMMARY OF DAMPING AND FREQUENCY DATA CYLINDRICAL
TANKS WITH INVERTED ELLIPSOIDAL BOTTOMS (Cont'd)

Tank Diameter (in.)	Liquid	N_{BO}	$N_{GA}^{-1/2}$	h/d	x_o (in.)	γ_s	f_1 (cps)	$(2\pi f_1)^2 \frac{R_o}{g}$	$(2\pi f_1^*)^2 \frac{R_o}{g}$
0.688	Methanol	26	0.0165	1.250	0.002	0.026	7.15	1.799	1.802
					0.003	0.027	7.08	1.764	1.768
				0.500	0.002	0.029	7.11	1.779	1.783
					0.003	0.027	7.08	1.764	1.765
0.383	CCl_4	14	0.0230	0.250	0.002	0.033	6.71	1.584	1.587
					0.003	0.030	6.67	1.565	1.568
				1.250	0.004	0.056	9.65	1.824	1.836
					0.500	0.003	0.039	9.60	1.805
			0.375	0.500	0.004	0.043	9.56	1.790	1.794
					0.375	0.005	0.043	9.25	1.676
				0.375	0.005	0.043	9.25	1.676	1.680

Note: $f_1^* = f_1 (1 - 2 \gamma_s^2)^{-1/2}$

purposes, the equation $\gamma_s = 0.83 N_{GA}^{-1/2}$, which is known to correlate damping data for large Bond numbers, is also shown. The present values of γ_s are substantially larger than this equation predicts, and the difference between the two increases as the Bond number decreases. ($\gamma_s = 0.83 N_{GA}^{-1/2}$ was originally formulated only for tanks with flat bottoms, but it should be valid when $h/d > 1.0$ for a cylindrical tank having any form of bottom. Further, the present definition of N_{GA} is the usual one employed for large Bond number tests and not the modified form, $N_{GA} = 4.62 \nu^{-1} R_{of}^2 f_1^*$, proposed in our Technical Report No. 5, Ref. [4]. The reasons for the change are that the difference between the two definitions for $N_{BO} > 10$ is small and that the numerical constant multiplying the form $\nu^{-1} R_{of}^2 f_1^*$ is a function of h/d .) To determine the kind of variation of γ_s with N_{BO} , the present data were compared to the correlation equation proposed in Technical Report No. 5, Ref. [4], which is

$$\gamma_s = 0.83 N_{GA}^{-1/2} (1 + 8.20 N_{BO}^{-3/5}) \quad (2)$$

The comparison is shown in Figure 9; it can be seen Eq. (2) does correlate the data very well.

The numerical constant A in the correlation equation $\gamma_s = A N_{GA}^{-1/2}$ is not known for large Bond numbers, and $h/d = 0.50$ or $h/d = 0.25$. But, by testing a number of different correlation equations, it was found that the experimental data could always be correlated by equations similar to Eq. (2). The best fit for $h/d = 0.50$ is given by

$$\gamma_s = 1.23 N_{GA}^{-1/2} (1 + 2.20 N_{BO}^{-3/5}) \quad (3)$$

while, for $h/d = 0.25$, it is

$$\gamma_s = 1.65 N_{GA}^{-1/2} (1 + 1.22 N_{BO}^{-3/5}) \quad (4)$$

These equations are shown plotted against the data in Figures 10 and 11; as can be seen, the correlation is fairly close.

As stated previously, the large Bond number correlation equations for tanks with inverted ellipsoidal bottoms are not known, but the ones for flat bottom tanks are given in Ref. [5], and they predict that the numerical constant which multiplies $N_{GA}^{-1/2}$ decreases slightly as h/d decreases. Here, however, the proportionally larger amount of viscous flow interference introduced by the inverted ellipsoidal bottom is reflected in an increase of the numerical constant as h/d decreases. Note, also, that the effect of N_{BO} is less for small than it is for large h/d . Furthermore, although Eqs. (2), (3), and (4) give a close correlation for the range of N_{BO} tested, they cannot be correct as $N_{BO} \rightarrow 0$ since they all predict that $\gamma_s \rightarrow \infty$, which is known not be the case [6].

IV. RESULTS FOR SPHERICAL TANKS

The objectives of this part of the program were the same as those for the cylindrical tank, namely, to measure the lateral slosh force and slosh damping as functions of the Bond number and the liquid depth. Because of fabrication requirements, the spherical tanks were machined from aluminum instead of from glass, and, for this reason, visual observations of the slosh behavior were impossible; nonetheless, the force response curves still indicate that here also the "free edge" condition held; likewise, the contact angle of the reagent grade liquids on the aluminum walls was still zero degrees.

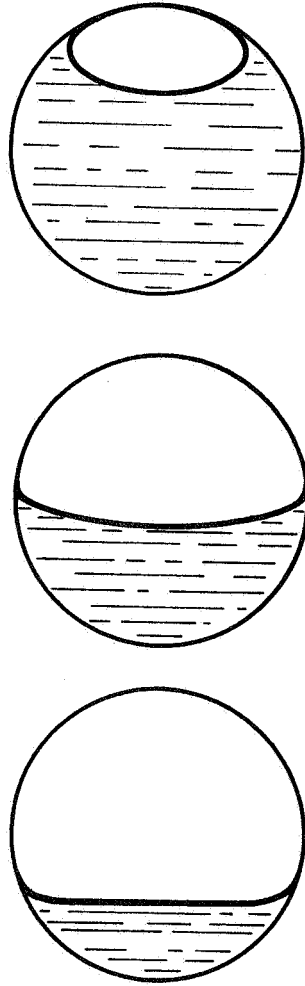
Since the amount of liquid contained in a spherical tank is less than that in a cylindrical tank of equal diameter and, consequently, the slosh forces are smaller and more difficult to measure, the smallest spherical tank used in the tests was 1.04-in. diameter. The lowest Bond number, however, was 43 instead of 60, which is the value obtained when N_{BO} is based on the tank diameter because the actual diameter of the free surface is always less than the tank diameter unless the tank is exactly half-full. (Basing the Bond number on the free surface diameter, and not on the tank diameter, is the proper way to define N_{BO} since the surface tension forces depend only on the size of the free surface and not on the size of the tank.) For both the 1.36 and the 1.04-in. diameter tank used in the tests, the liquid depth-to-tank diameter ratios were always 3/4, 1/2, or 1/4†. Table II gives the necessary information for converting h_{av}/d to the ratio of free surface diameter (d_{fs}) to tank diameter (d) and to percent fullness of the tank.

TABLE II. DIAMETER OF FREE SURFACE AND PERCENTAGE FULLNESS OF TANK

<u>h_{av}/d</u>	<u>d_{fs}/d</u>	<u>% Full</u>
0.25	0.866	15.6
0.50	1.000	50.0
0.75	0.888	84.4

*Because measurements of the liquid depth below the meniscus could not be obtained here, the "liquid depth" for spherical tanks is the average depth, h_{av} , the distance from the tank bottom to a hypothetical, flat, free surface enclosing the same actual liquid volume as used in the tests.

Even though the Bond numbers for $h_{av}/d = 0.25$ and 0.75 are the same, the curvature of the free surface for $h_{av}/d = 0.75$ is greater than for $h_{av}/d = 0.25$ (as shown in the following sketch) because of the necessity



of maintaining the condition of zero-degree contact angle. Thus, the same Bond number might be expected to have different effects for different liquid levels.

A. Force Response

Figures 12 through 16 show typical force response curves for CCl_4 , methanol, and acetone. (The Bond number of CCl_4 in the 1.04-in. diameter tank is the same as that for methanol or acetone in the 1.36-in. diameter tank; thus, the results for CCl_4 in this tank are not shown, although the natural frequency and slosh damping were determined and will be discussed later.) The solid lines in the figures are faired curves through the experimental data, and, once again, the curves have not been

nondimensionalized in any way. Note that the forces for $h_{av}/d = 0.25$ are always shown at twice the indicated scales since otherwise these curves would be too small to be legible.

The range of Bond numbers covered in the figures is 175 (CCl_4 in 1.36-in. tank, $h_{av}/d = 0.50$) to 43 (acetone in 1.04-in. tank, $h_{av}/d = 0.25$ or 0.75). Other data given in the figure include the amplitude of tank excitation (x_o , inches), the resonant frequency (f_1 , cps), and the slosh damping coefficient (γ_s). Because the slosh wave could not be observed visually, the wave height at resonance could not be determined.

The force response, once again, is reasonably linear. It can be seen that the largest forces for any given tank, liquid, and x_o always occur for $h_{av}/d = 0.50$, which is in agreement with large Bond number results; this is caused by the slosh mass in the equivalent mechanical model having its largest value at $h_{av}/d = 0.50$. The absolute magnitudes of the peak slosh forces were compared with the predictions of the large Bond number mechanical model given in Ref. [5]†, and it was found that the experimental forces agreed to within $\pm 10\%$ of the large N_{BO} predictions; this is also approximately the change in slosh force experienced in cylindrical tanks when going from large to moderately small Bond numbers. There is, as yet, no theory for small Bond number sloshing in spherical tanks, and, thus, these experimental conclusions cannot be checked.

The response curves, while reasonably linear, are not quite so linear as the similar curves for cylindrical tanks. Further, for $h_{av}/d = 0.75$, the curves are nonlinear softening, while, for $h_{av}/d = 0.25$, they are nonlinear hardening (i.e., the resonant frequency increases with excitation amplitude for $h_{av}/d = 0.25$).

B. Natural Frequency

The resonant frequencies determined from the force response curves were corrected for the effects of damping by the same method as described in Section III. The results for all the tests are shown in the last column of Table III, as well as graphically in Figure 17 for the smallest x_o whenever a choice existed. The natural frequency parameters for $N_{BO} = \infty$ and $h/d = 0.75$, 0.50, and 0.25 are also shown on this figure for purposes of comparison. The solid lines in the figure are faired curves through the test data.

†The label on the slosh mass curve in Figure 6.7 of [5] is incorrect, as is also the original curve in the reference from which the figure was adapted; instead of m_1/m_T , the curve should be labeled m_1/m_{FULL} .

It can be seen that the data points are consistent since, for equal Bond numbers, the experimental values of $(2\pi f_1^*)^2 R_o/g$ obtained with any of the liquid-tank combinations are very nearly the same. But, the same Bond number has a significantly different effect for different liquid levels. This can be understood in terms of the free surface curvature and the surface tension; for the same curvature, an increase in surface tension increases the natural frequency, but, for the same surface tension, an increase in free surface curvature decreases the natural frequency, which may be deduced from the theory given for cylindrical tanks in Ref. [2]. Since the curvature of the free surface in a spherical tank increases as the liquid level increases while (for the same liquid) the surface tension is constant, the effect of free surface curvature on the natural frequency increases as the liquid level increases. In the case of $h_{av}/d = 0.25$, the effects of curvature and surface tension appear nearly to balance over the entire range of Bond numbers considered so that $(2\pi f_1^*)^2 R_o/g$ is nearly constant and independent of N_{BO} . For $h_{av}/d = 0.75$, however, the curvature effects predominate so that the natural frequency decreases as the Bond number decreases; in fact, for $N_{BO} = 45$, the natural frequency parameter is about 20% less than the large Bond number frequency calculated for the same R_o and g . This is about twice the change found in cylindrical tanks for the same N_{BO} ; furthermore, the frequency in spherical tanks is never greater than the large Bond limit, which also is in contrast to the results from cylindrical tanks. Nonetheless, for very small N_{BO} , the curves must slope upward and approach infinity; otherwise, a value of f_1^* equal to zero would be predicted as $g \rightarrow 0$. Such small values of N_{BO} are completely out of the range of the present tests.

C. Slosh Damping

The slosh damping coefficient γ_s for all the tests with spherical tanks was determined by the half-bandwidth technique; the results are shown in the seventh column of Table III. The results show that in every case the minimum damping is obtained when the tank is half-full: $h_{av}/d = 0.50$. Further, the damping coefficient for $h_{av}/d = 0.25$ is always the largest and is, for any given tank and liquid, about 50% larger than the damping for $h_{av}/d = 0.75$, which in turn is about 10 to 20% larger than the damping for $h_{av}/d = 0.50$. Similar results have been found for large Bond number sloshing in spherical tanks [5], but, in that case, γ_s for $h_{av}/d = 0.75$ and 0.25 were about equal; thus, once again, the effects of the differences in free surface curvature for $h_{av}/d = 0.75$ and 0.25 for small Bond number sloshing are evident.

It is also evident from Table III that, generally, γ_s increases both as $N_{GA}^{-1/2}$ increases or as N_{BO} decreases. However, the range of $N_{GA}^{-1/2}$ and N_{BO} is not large enough to determine a correlation equation for these data. Several equations were attempted, but none seemed to fit the

TABLE III. SUMMARY OF DAMPING AND FREQUENCY
DATA SPHERICAL TANKS

Tank Diameter (in.)	Liquid	$N_{GA}^{-1/2}$	N_{BO}	h_{av}/d	x_o (in.)	γ_s	f_1 (cps)	$(2\pi f_1)^2 \frac{R_o}{g}$	$(2\pi f_1^*)^2 \frac{R_o}{g}$
1.36	CCl_4	0.0089	131	1/4	0.002	0.019	4.11	1.176	1.176
					0.003	0.018	4.10	1.170	1.170
					0.004	0.017	4.09	1.165	1.165
			175	1/2	0.002	0.013	4.63	1.493	1.493
					0.003	0.012	4.61	1.480	1.480
			131	3/4	0.002	0.014	5.41	2.038	2.038
1.36	Methanol	0.0099	75	1/4	0.0015	0.027	4.10	1.170	1.171
					0.002	0.025	4.10	1.170	1.171
					0.003	0.021	4.12	1.182	1.183
			100	1/2	0.002	0.014	4.62	1.486	1.486
					0.003	0.015	4.60	1.473	1.473
			75	3/4	0.002	0.019	5.35	1.993	1.995
1.36	Acetone	0.0074	73	1/4	0.002	0.015	4.08	1.159	1.159
			98	1/2	0.002	0.009	4.58	1.461	1.461
			73	3/4	0.002	0.011	5.27	1.934	1.934
					0.002	0.029	4.68	1.166	1.167
			75	1/4	0.003	0.029	4.70	1.176	1.177
					0.002	0.018	5.25	1.468	1.469
1.04	CCl_4	0.0109	100	1/2	0.003	0.016	5.24	1.462	1.463
			75	3/4	0.002	0.022	6.11	1.988	1.990
					0.003	0.020	6.01	1.923	1.925

TABLE III. SUMMARY OF DAMPING AND FREQUENCY
DATA SPHERICAL TANKS (Cont'd)

Tank Diameter (in.)	Liquid	$N_{GA}^{-1/2}$	N_{BO}	h_{av}/d	x_o (in.)	γ_s	f_1 (cps)	$(2\pi f_1)^2 \frac{R_o}{g}$	$(2\pi f_1)^2 \frac{R_o}{g}$
1.04	Methanol	0.0121	45	1/4	0.003	.030	4.67	1.161	1.163
			60	1/2	0.003	.019	5.21	1.445	1.446
1.04	Acetone	0.0090	45	3/4	0.002	.024	5.90	1.854	1.856
					0.003	.025	5.86	1.829	1.831
			43	1/4	0.003	.020	4.65	1.151	1.152
			57	1/2	0.002	.011	5.20	1.440	1.440
					0.003	.012	5.15	1.412	1.412
			43	3/4	0.002	.012	5.82	1.804	1.804

Note: $f_1 = f_1^* (1 - 2\gamma_s^2)^{-1/2}$

data as well as the corresponding equations for cylindrical tanks given in Section III. Regardless of this, the damping factor in larger tanks can be estimated for constant N_{BO} by modifying the data in Table III according to $N_{GA}^{-1/2}$ scaling; that is, the damping in a large tank is approximately

$$(\gamma_s)_{\text{large}} = \frac{(N_{GA}^{-1/2})_{\text{large}}}{(N_{GA}^{-1/2})_{\text{small}}} (\gamma_s)_{\text{small}} \quad (5)$$

when N_{BO} in the large tank is the same as in the small tanks used in our tests.

V. CONCLUSIONS

The results of the experimental program with cylindrical tanks having ellipsoidal bottoms show that the sloshing behavior for small Bond numbers is qualitatively similar to that occurring for very large Bond numbers. The main differences between the two types of sloshing are: (1) the natural frequency for small N_{BO} sloshing increases as N_{BO} decreases; and (2) the damping coefficient, γ_s , is larger for small N_{BO} than for large N_{BO} sloshing. It was found that the damping coefficient could be computed with sufficient accuracy by

$$\gamma_s = 0.83 N_{GA}^{-1/2} (1 + 8.20 N_{BO}^{-3/5}); h/d \geq 1.25$$

$$\gamma_s = 1.23 N_{GA}^{-1/2} (1 + 2.20 N_{BO}^{-3/5}); h/d = 0.50$$

$$\gamma_s = 1.65 N_{GA}^{-1/2} (1 + 1.22 N_{BO}^{-3/5}); h/d = 0.25$$

The spherical tank results were also in qualitative agreement with large Bond number sloshing. Here, however, the natural frequency decreases as N_{BO} decreases (in the range $N_{BO} > 43$) because of free surface curvature effects that are accentuated for liquid depths greater than one-half the diameter; in fact when $h_{av}/d = 0.75$, the natural frequency for $N_{BO} \approx 45$ is 20% less than the natural frequency for $N_{BO} = \infty$. The slosh mass in the equivalent mechanical model also varies with N_{BO} , although, in the present tests, the variation was never more than about $\pm 10\%$ of the large N_{BO} value.

There are, at present, no theoretical results available to compare with our experimental data. These theories, however, would be very useful in understanding the experimental results, especially as concerns spherical tanks in which significant differences between small and large N_{BO} sloshing are evident, even for $N_{BO} \approx 45$. It is recommended that such theories, therefore, be developed in the near future.

LIST OF REFERENCES

1. Satterlee, H. M. and Reynolds, W. C., "The Dynamics of the Free Liquid Surface in Cylindrical Containers under Strong Capillary and Weak Gravity Conditions," Tech. Rept. No. LG-2, Dept. of Mech. Eng., Stanford University, May 1, 1964.
2. Dodge, F. T. and Garza, L. R., "Experimental and Theoretical Studies of Liquid Sloshing at Simulated Low Gravities," Tech. Rept No. 2, Contract NAS8-20290, Southwest Research Institute, San Antonio, Texas, October 1966. (Also, Trans. ASME, J. Applied Mech., 34, Series E, No. 3, pp. 555-562, September 1967.)
3. Clark, L. V. and Stephens, D. G., "Simulation and Scaling of Low-Gravity Slosh Frequencies and Damping," AIAA Space Simulation Symposium Preprint, Philadelphia, Pennsylvania, September 1967.
4. Dodge, F. T. and Garza, L. R., "Simulated Low-Gravity Sloshing in Cylindrical Tanks Including Effects of Damping and Small Liquid Depth," Tech. Rept. No. 5, Contract NAS8-20290, Southwest Research Institute, San Antonio, Texas, December 1967.
5. The Dynamic Behavior of Liquids in Moving Containers, ed. H. N. Abramson, NASA SP-106 (1966).
6. Salzman, J. A., Labus, T. L., and Masica, W. J., "An Experimental Investigation of the Frequency and Viscous Damping of Liquids During Weightlessness," NASA TN D-4132 (1967).

APPENDIX
ILLUSTRATIONS

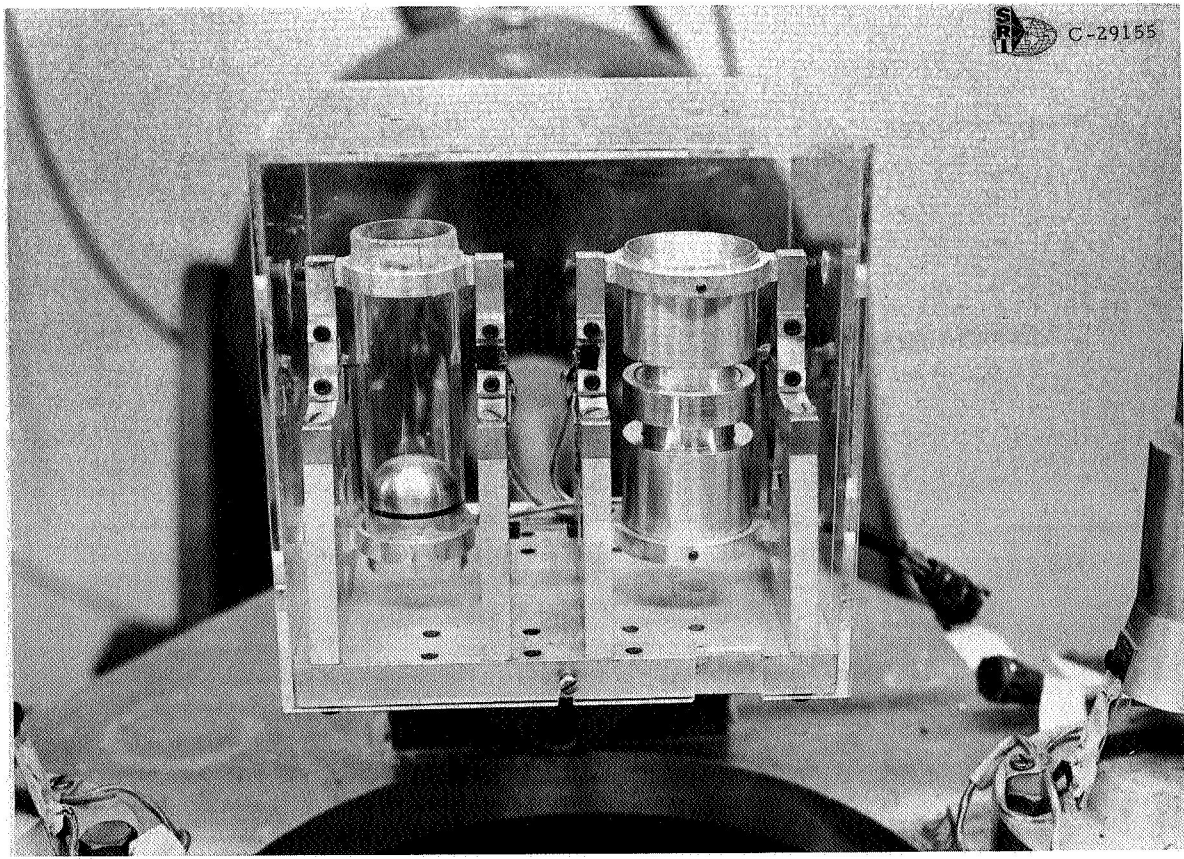
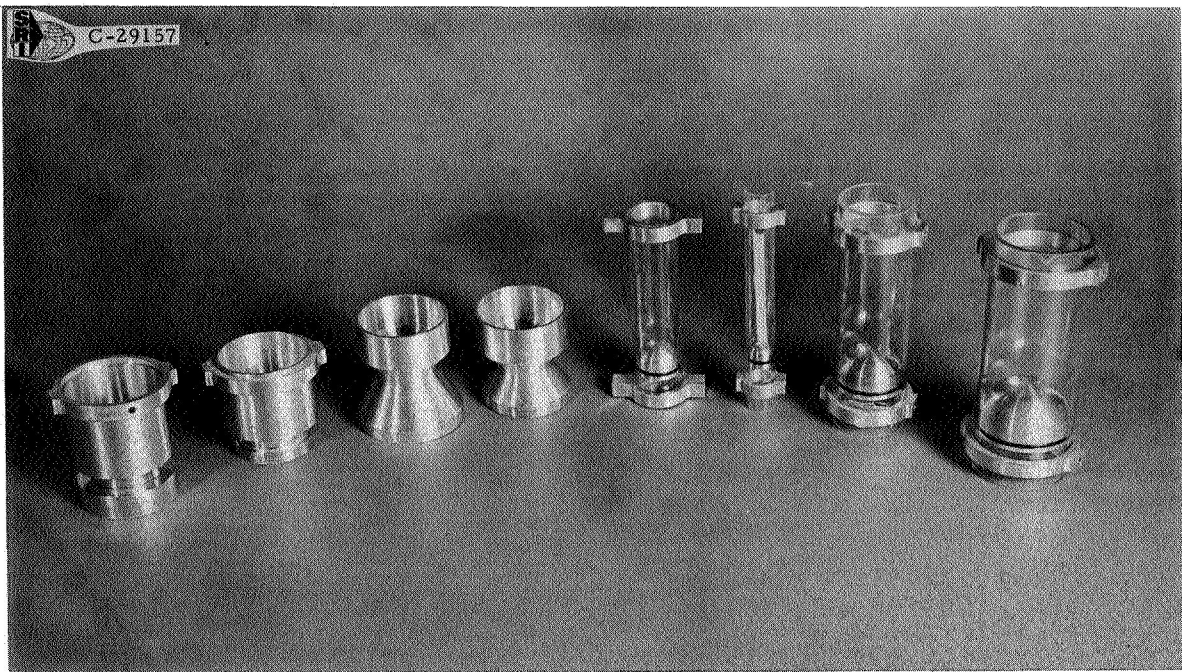


Figure 1. Tanks And Dynamometer Used In Tests

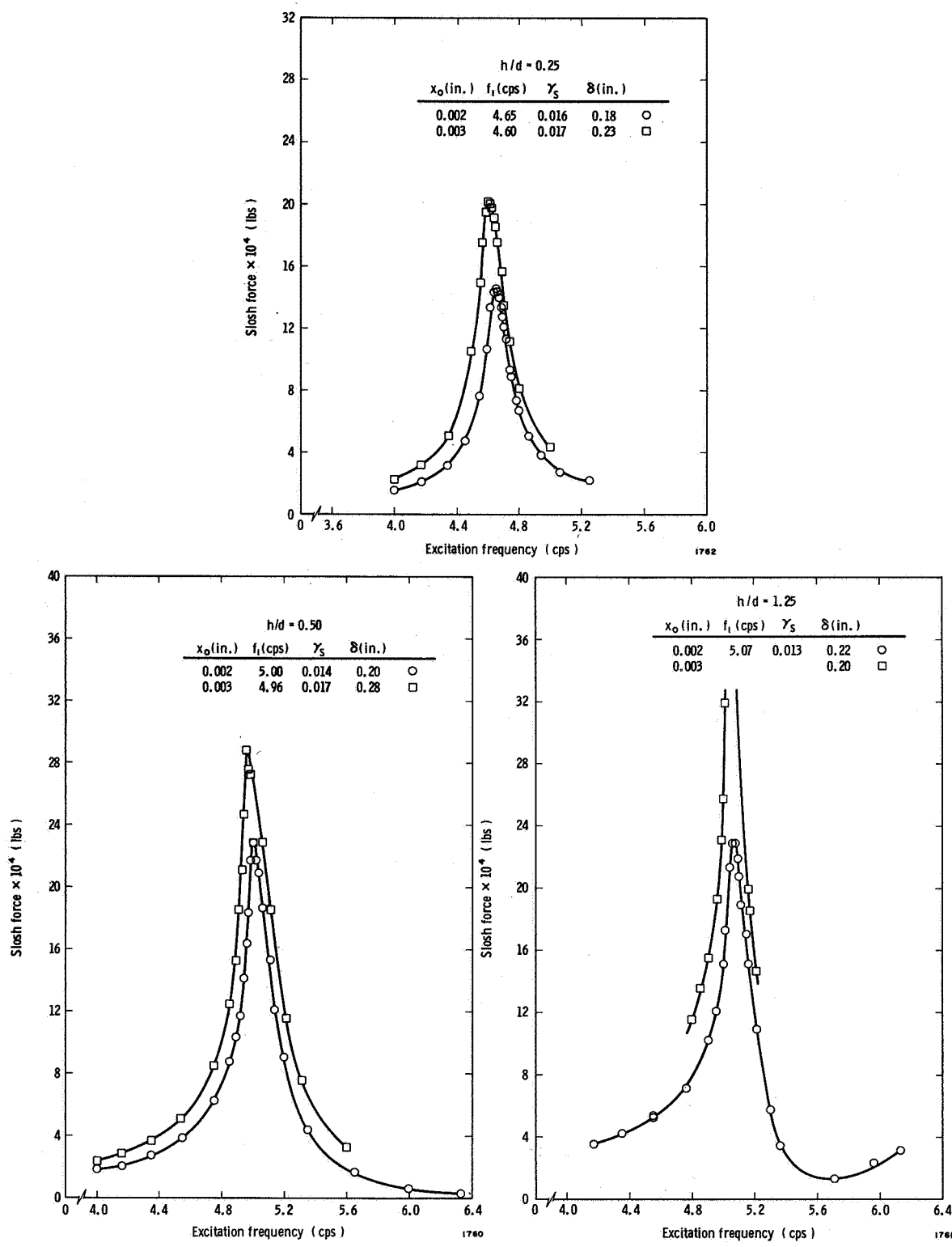


Figure 2. Force Response Curves For Methanol In 1.36" Cylindrical Tank, $N_{BO} = 100$

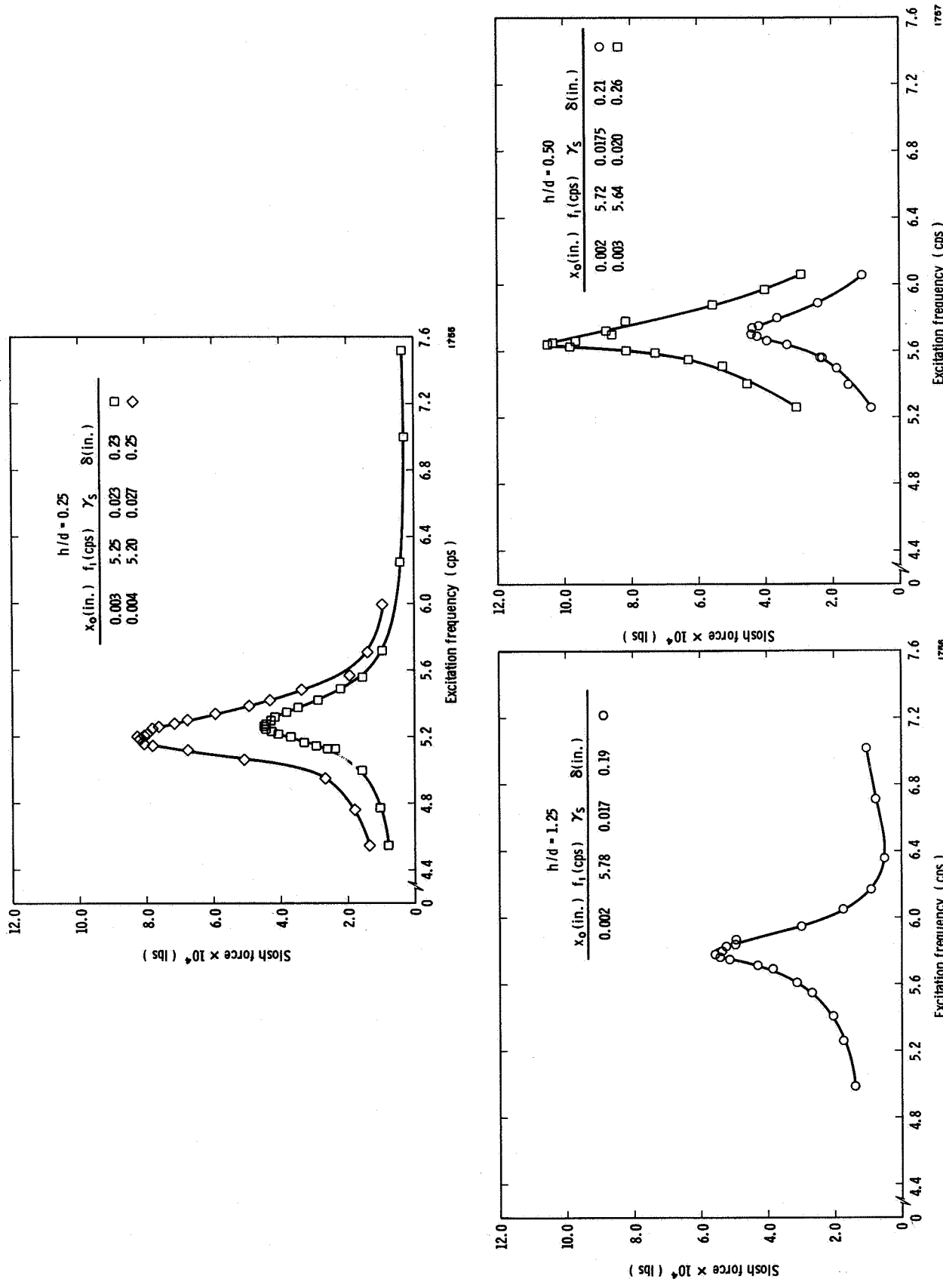


Figure 3. Force Response Curves For Methanol In 1.04" Cylindrical Tank, $N_{BO} = 60$

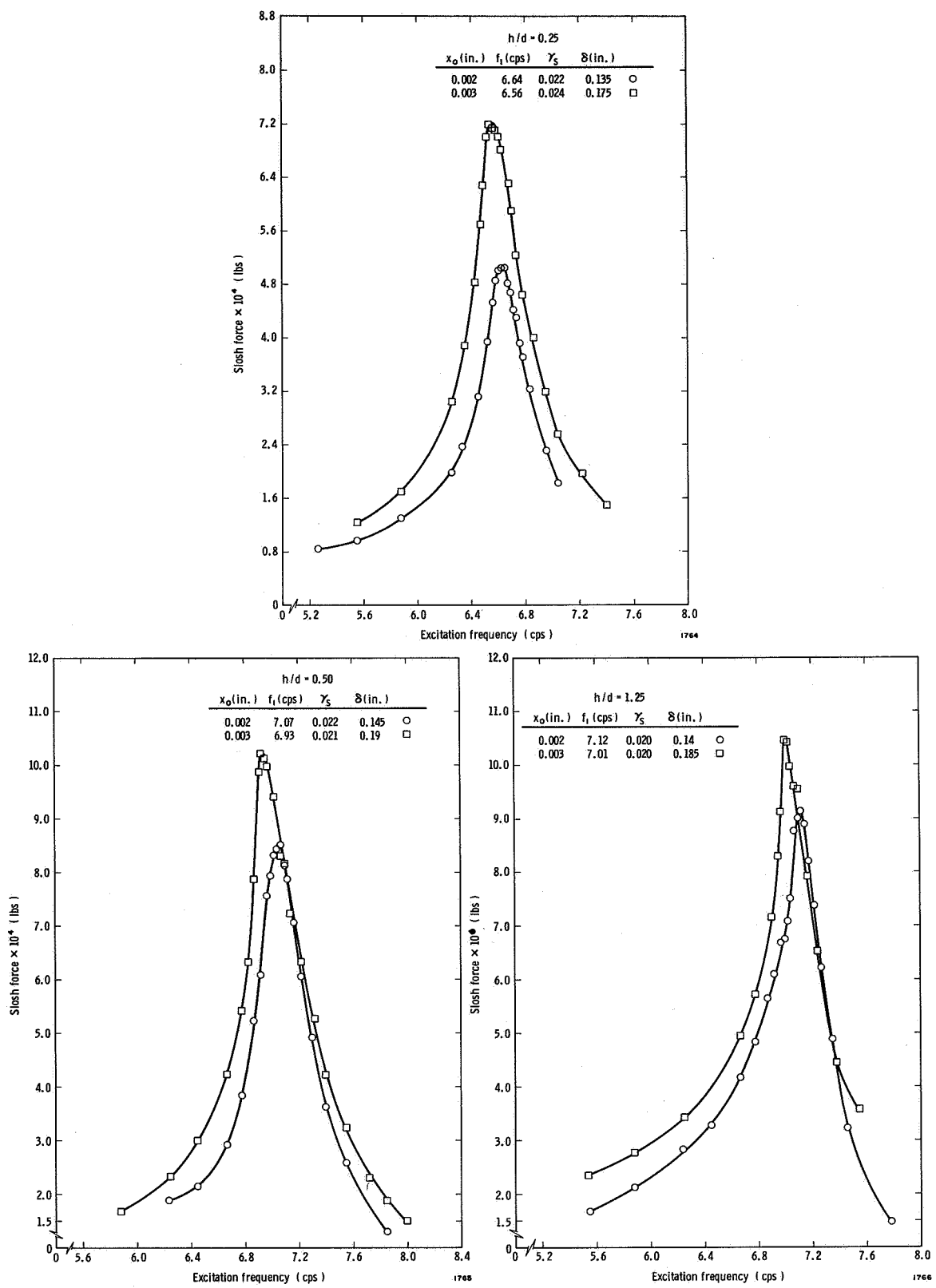


Figure 4. Force Response Curves For CCl_4 In 0.688"
Cylindrical Tank, $N_{\text{BO}} = 45$

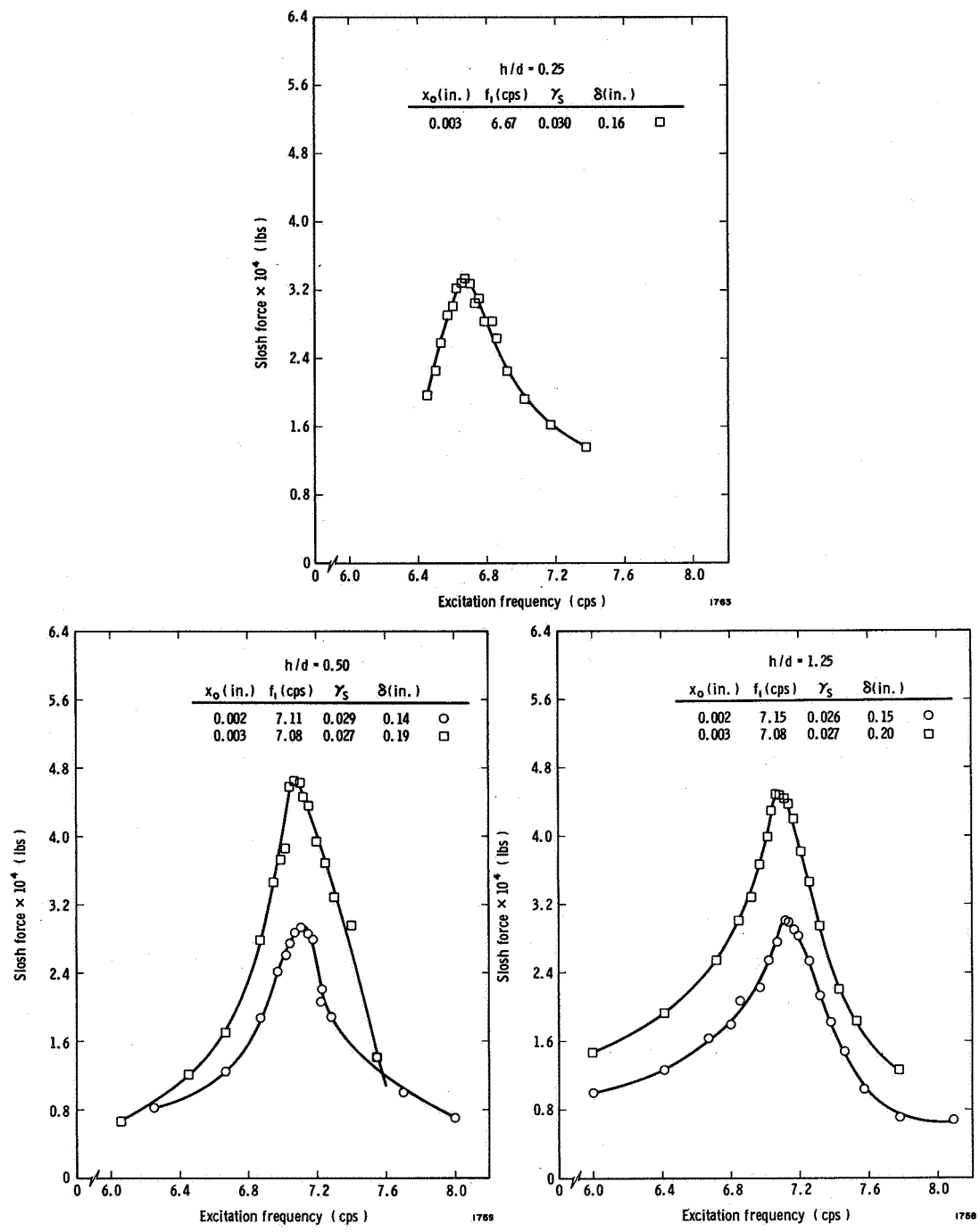


Figure 5. Force Response Curves For Methanol In 0.688" Cylindrical Tank, $N_{BO} = 26$

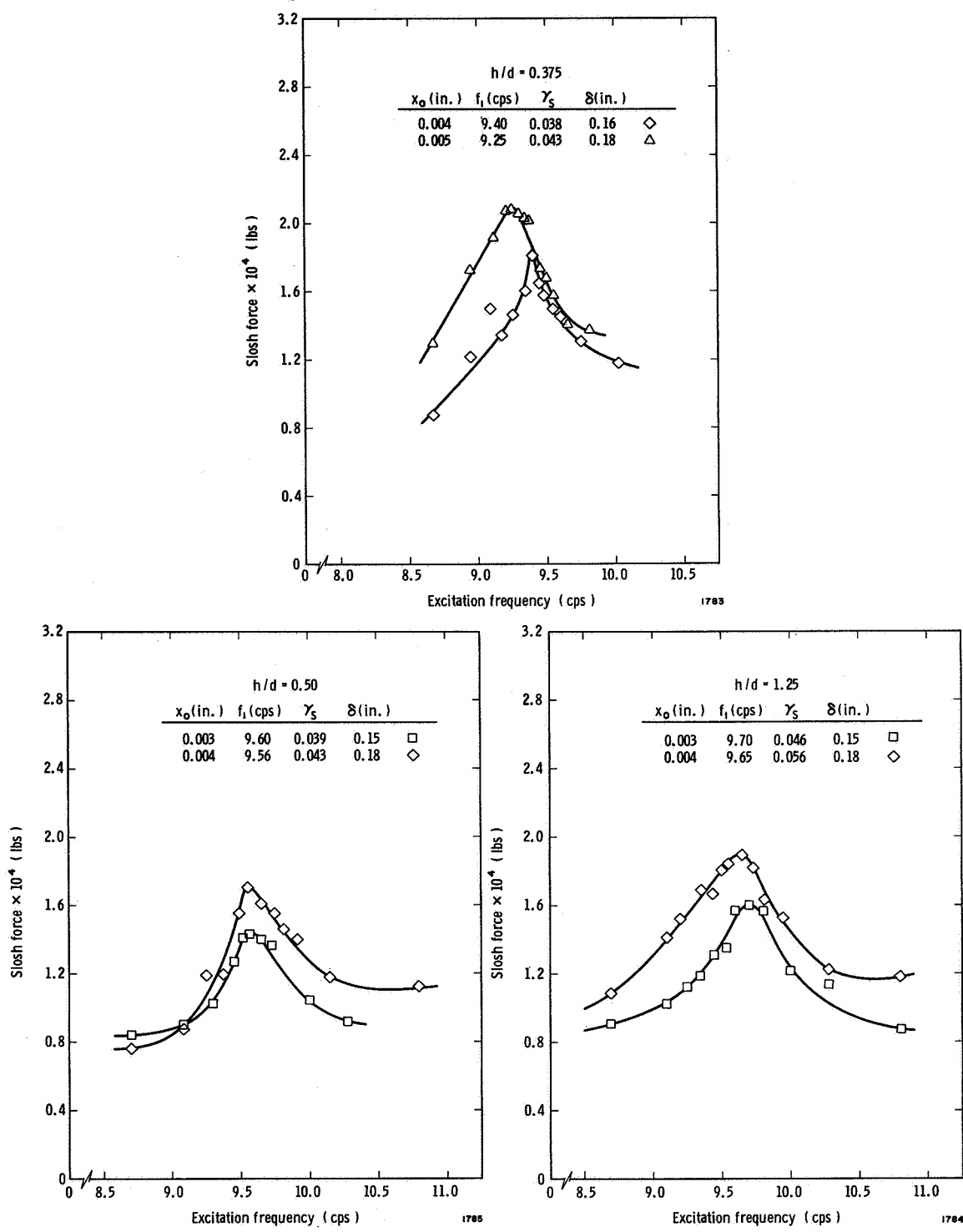


Figure 6. Force Response Curves For CCl_4 In 0.383" Cylindrical Tank, $N_{\text{BO}} = 14$

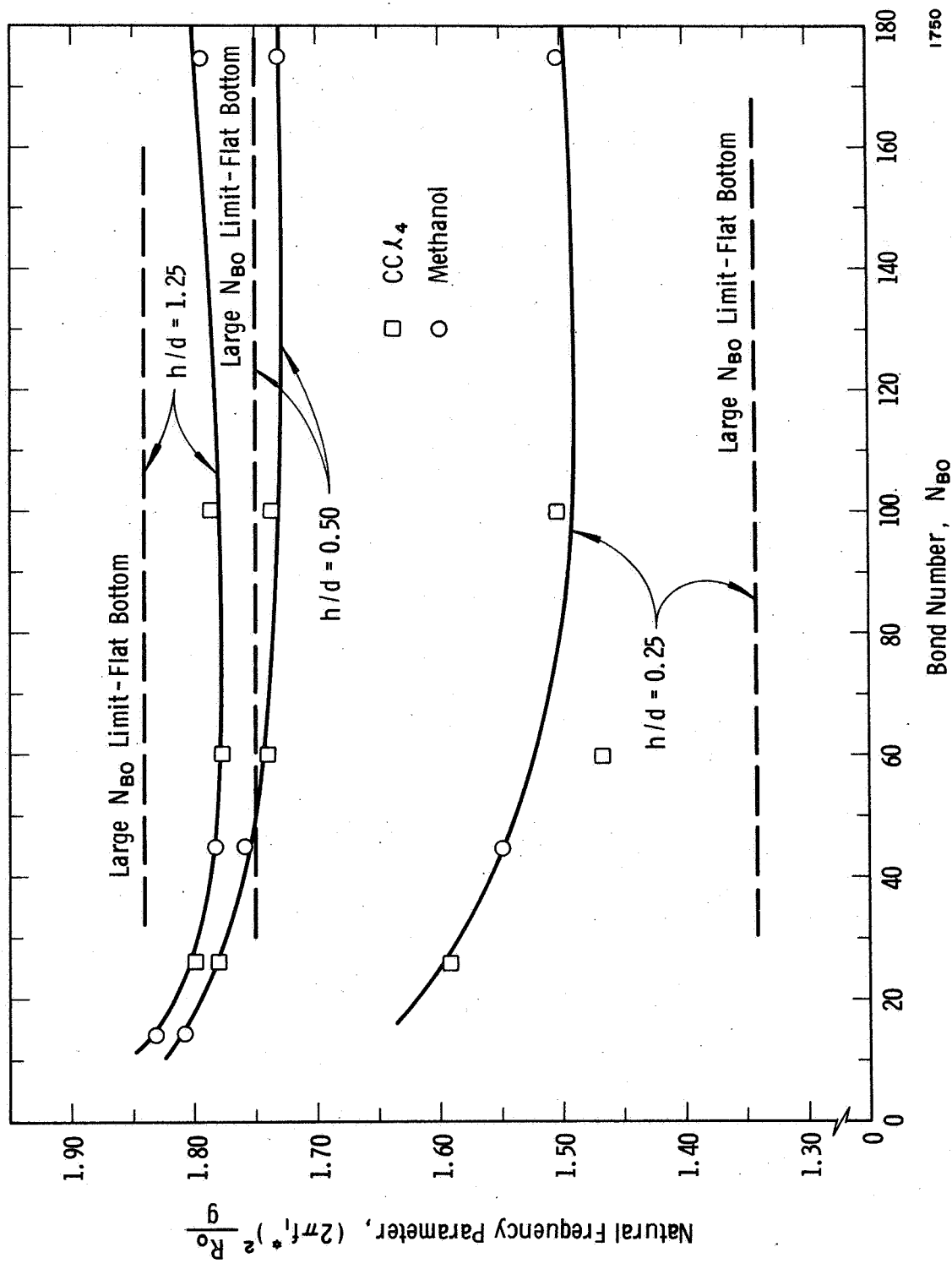


Figure 7. Variation Of Natural Frequency Parameter \ln Cylindrical Tanks With Bond Number

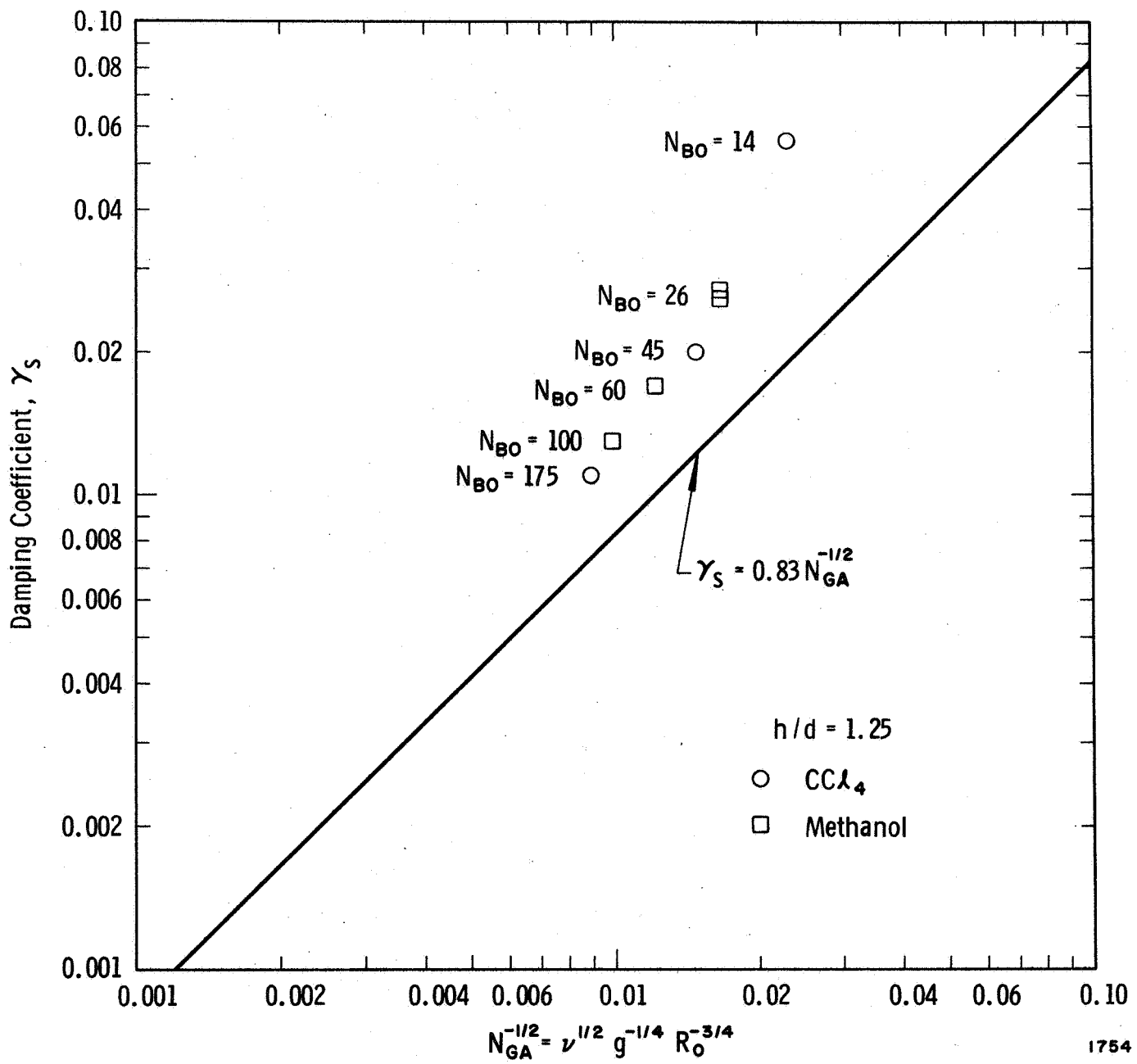


Figure 8. Variation Of Damping Coefficient With Galileo Number, $h/d = 1.25$

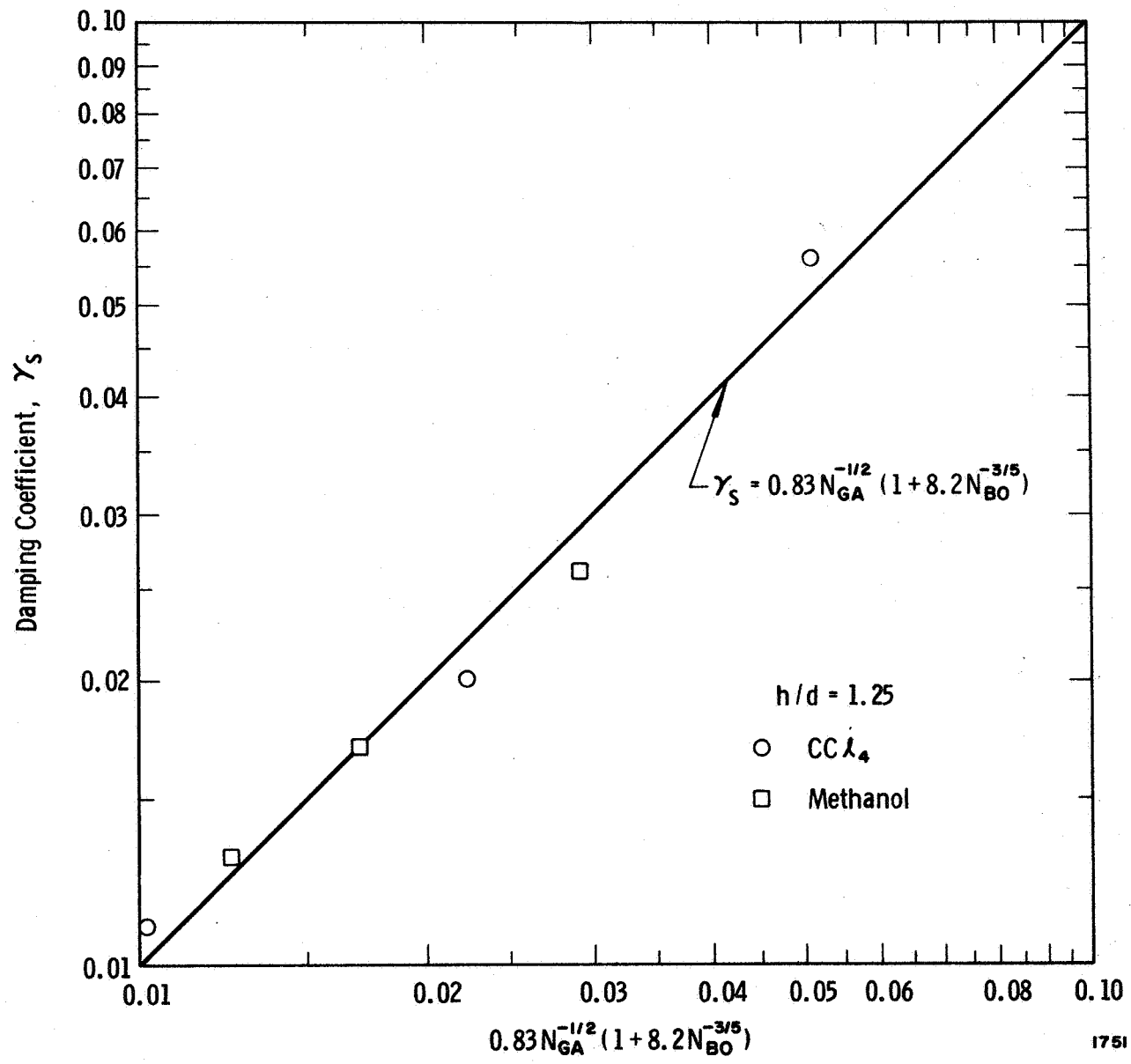


Figure 9. Damping Coefficient vs $0.83 N_{GA}^{-1/2} (1 + 8.2 N_{BO}^{-3/5})$, $h/d = 1.25$

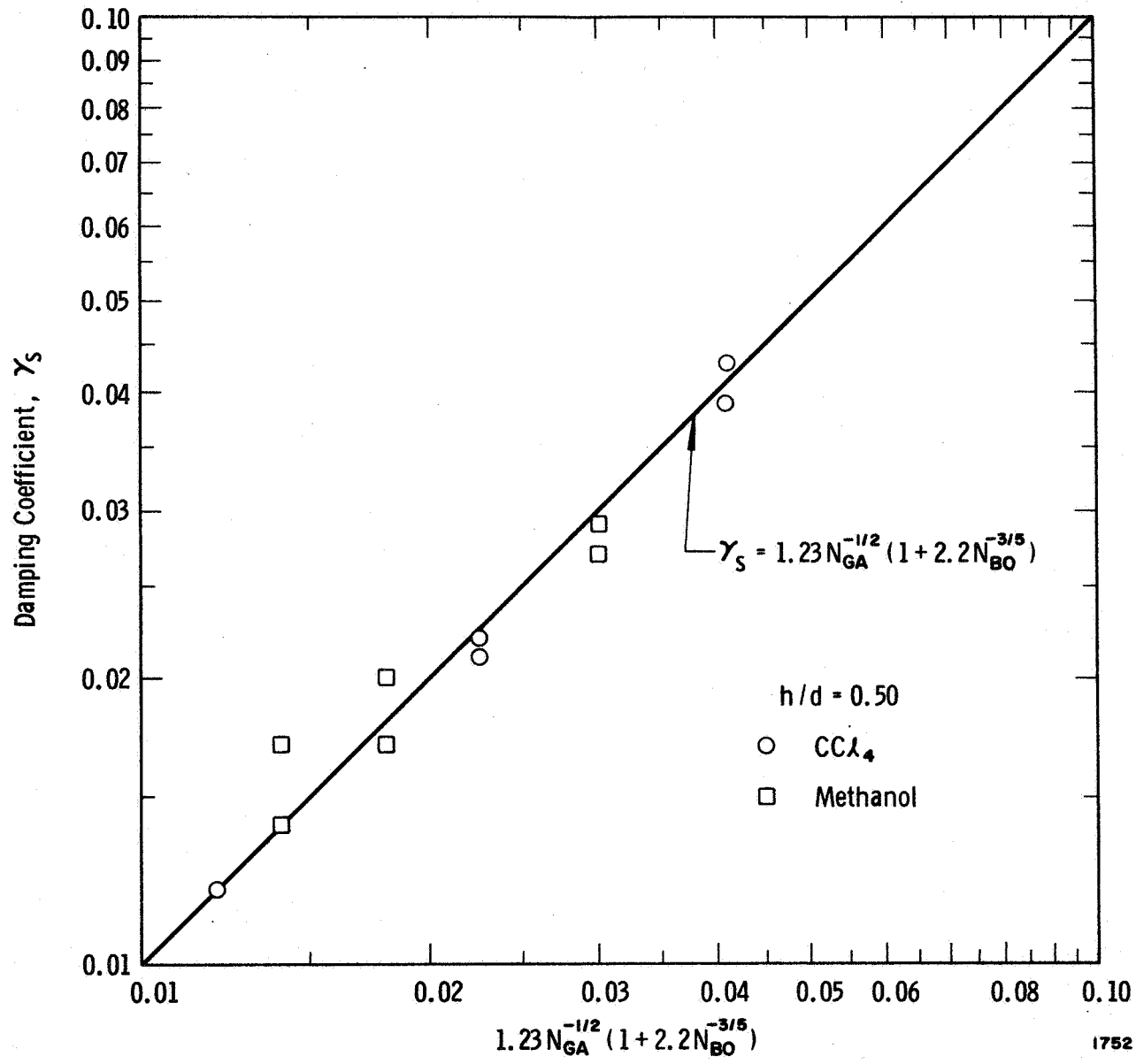


Figure 10. Damping Coefficient vs $1.23 N_{GA}^{-1/2} (1 + 2.2 N_{BO}^{-3/5})$, $h/d = 0.50$

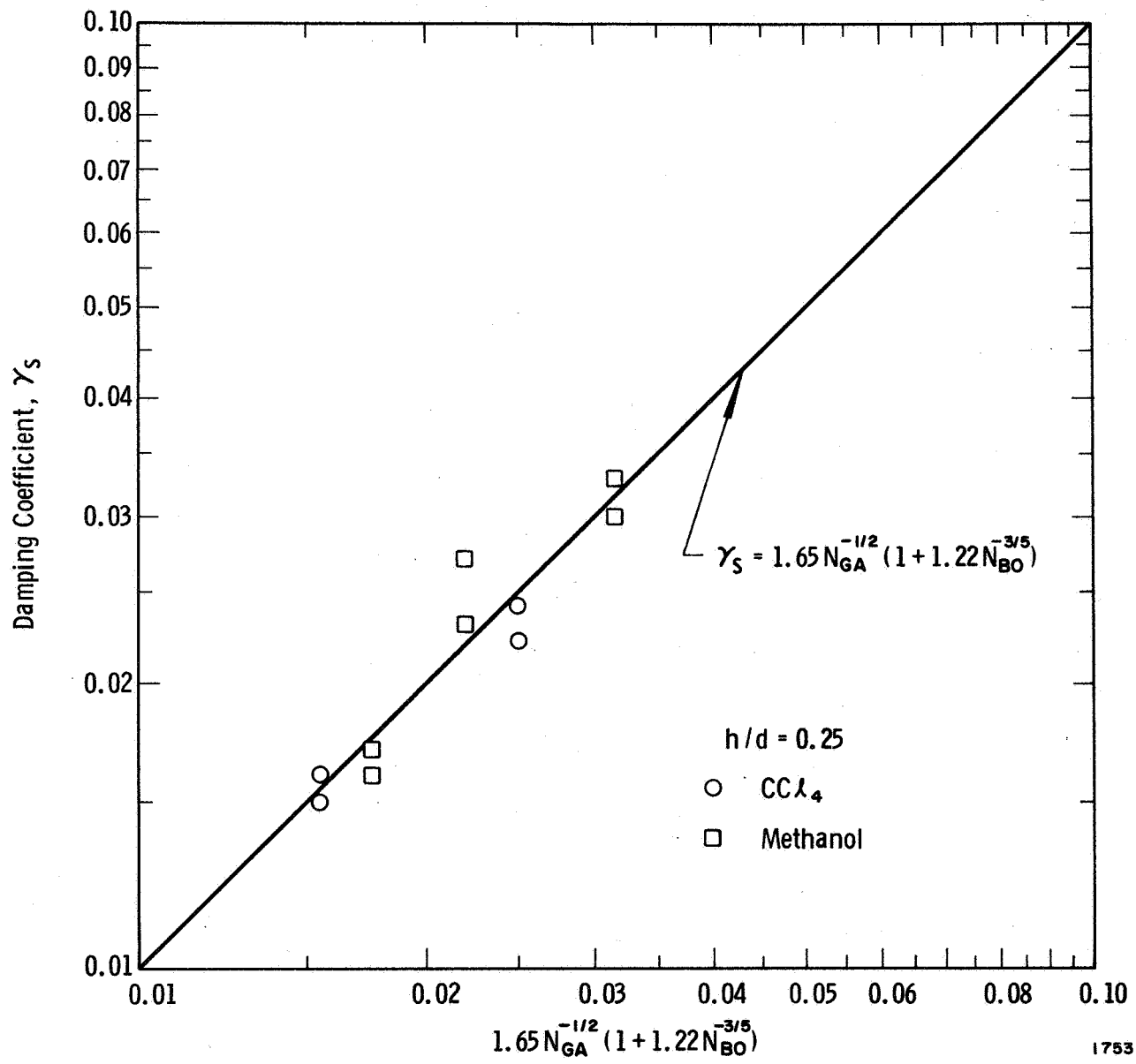
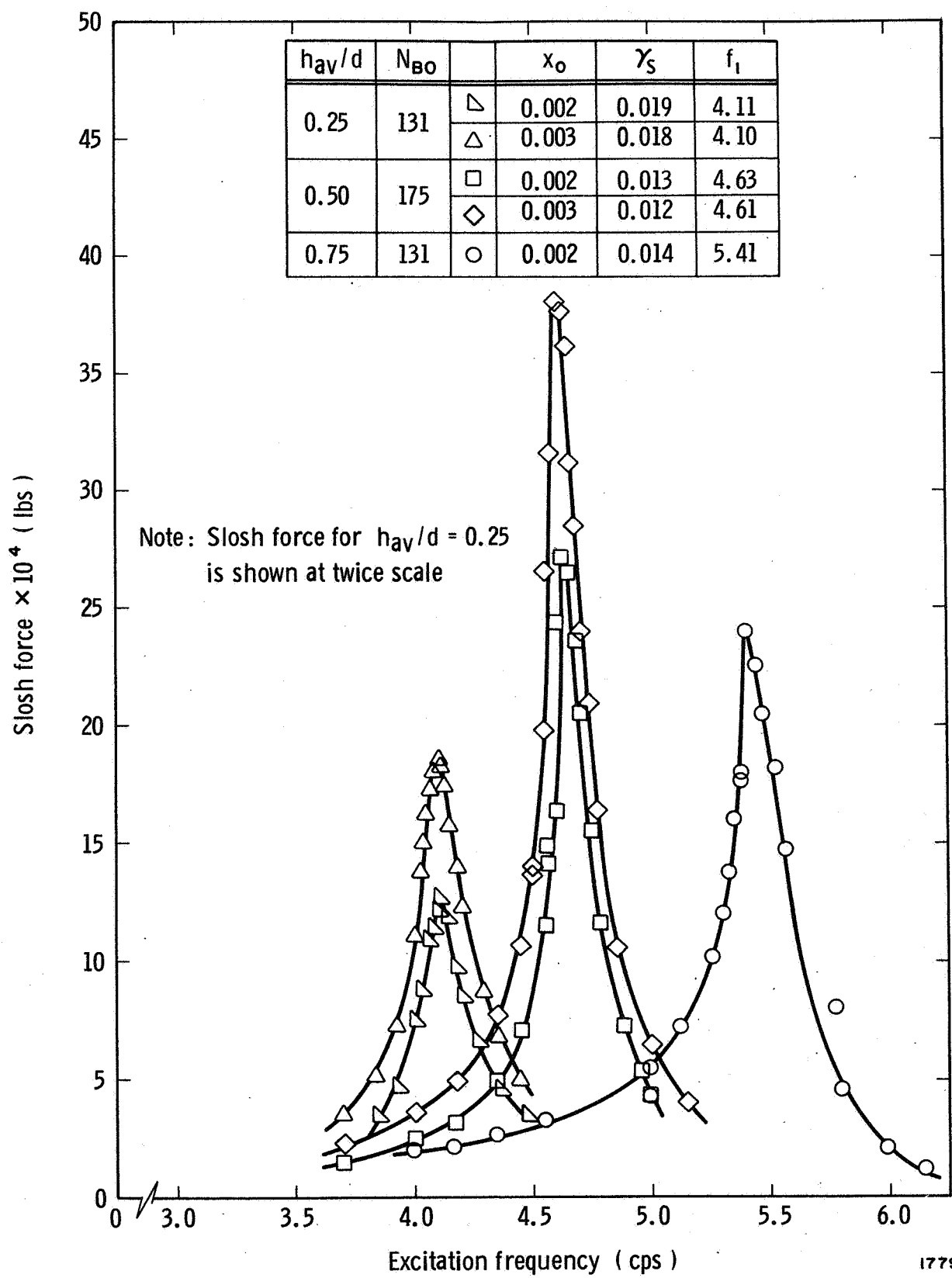


Figure 11. Damping Coefficient vs $1.65 N_{GA}^{-1/2} (1 + 1.22 N_{BO}^{-3/5})$, $h/d = 0.25$

1753

Figure 12. Force Response Curves $CCCL_4$ in 1.36" Spherical Tank

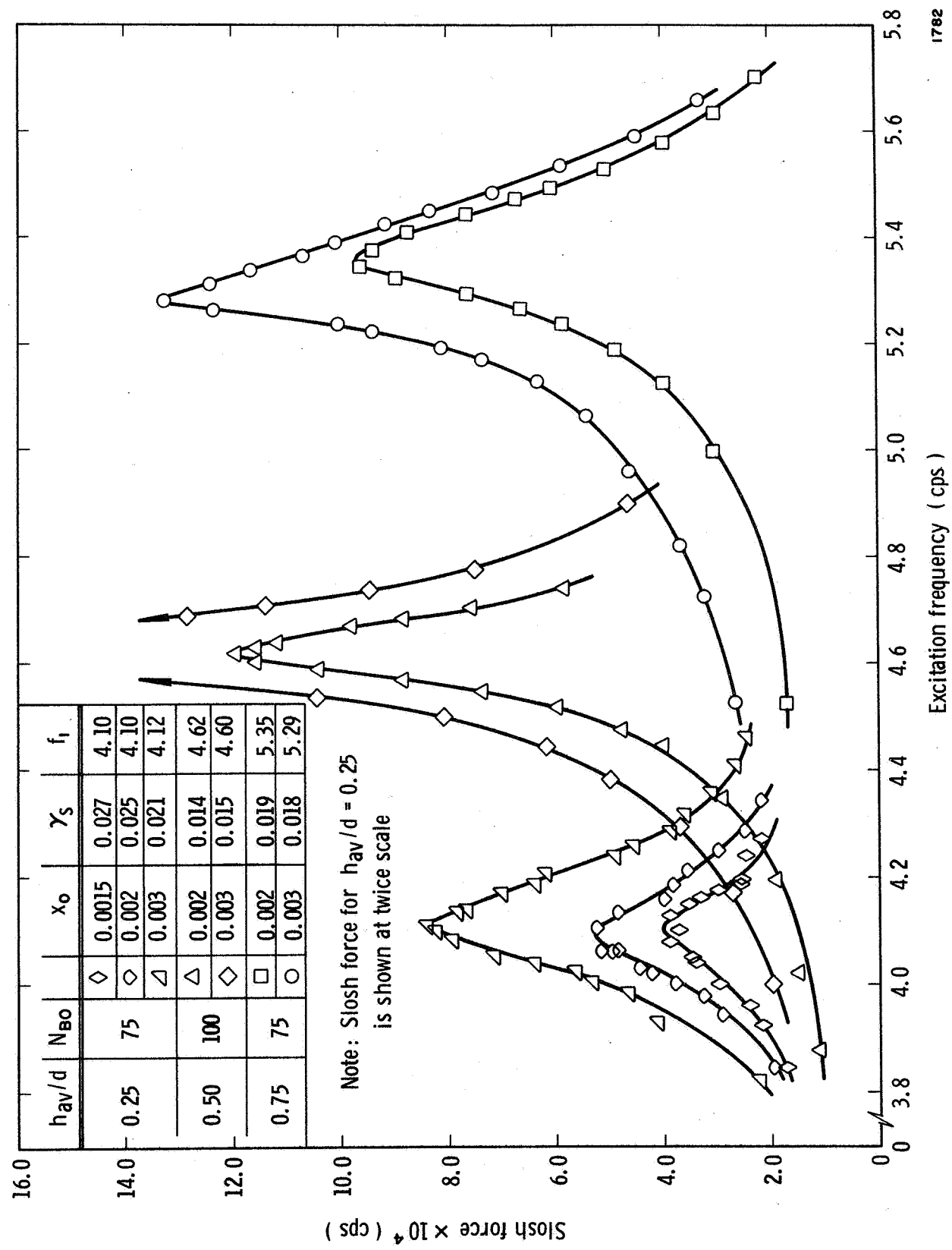


Figure 13. Force Response Curves For Methanol In 1.36" Spherical Tank

1782

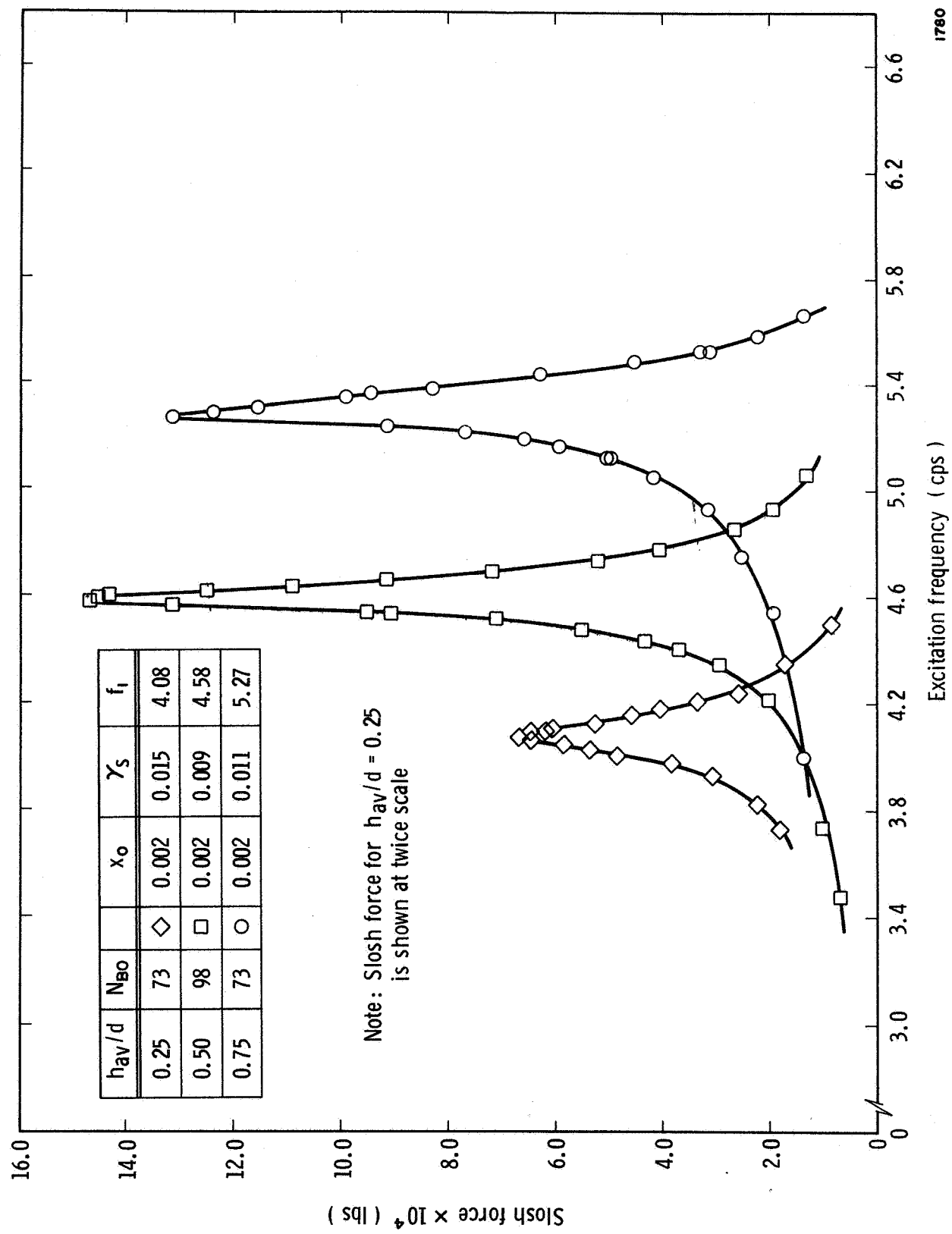


Figure 14. Force Response Curves For Acetone In 1.36" Spherical Tank

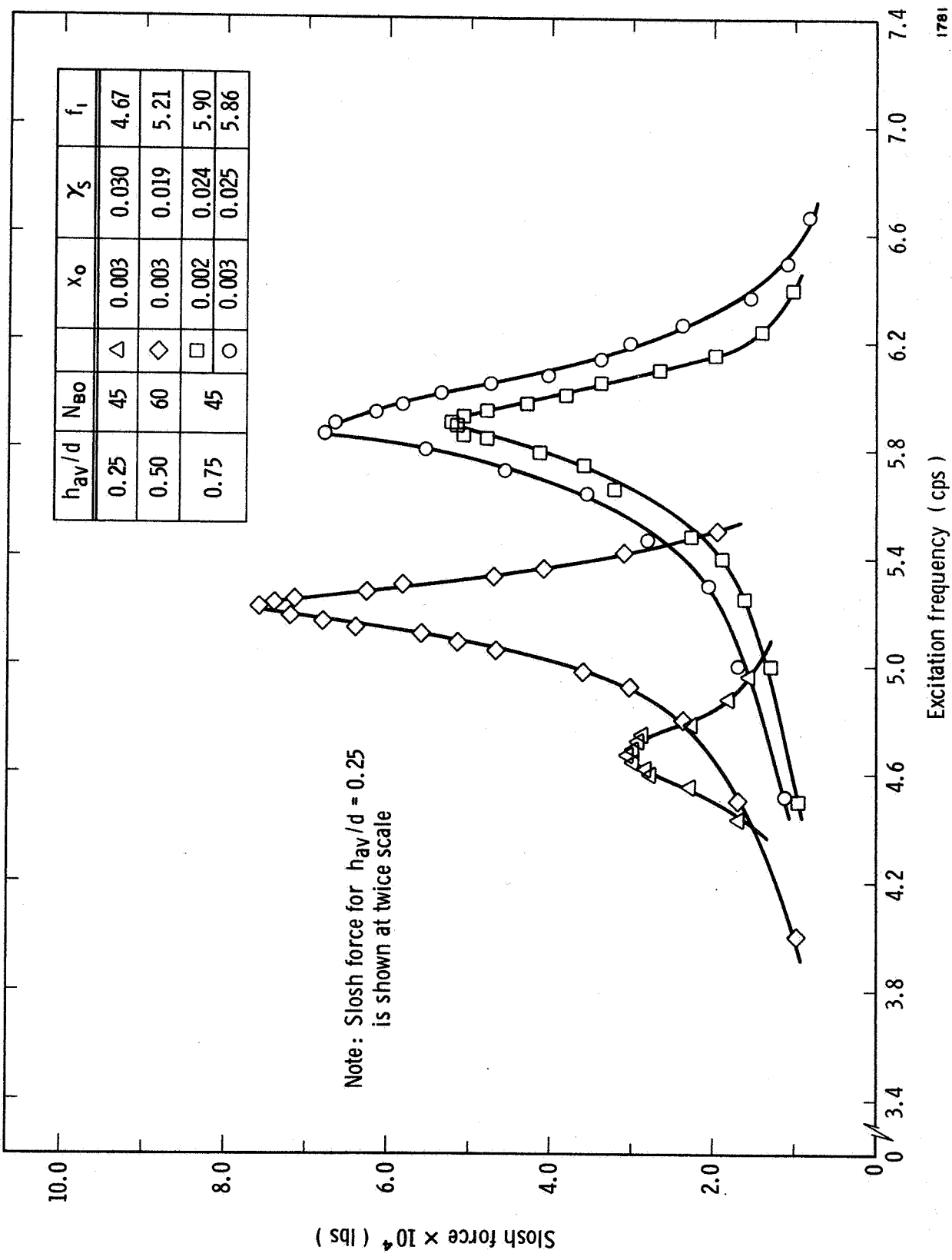


Figure 15. Force Response Curves For Methanol In 1.04" Spherical Tank

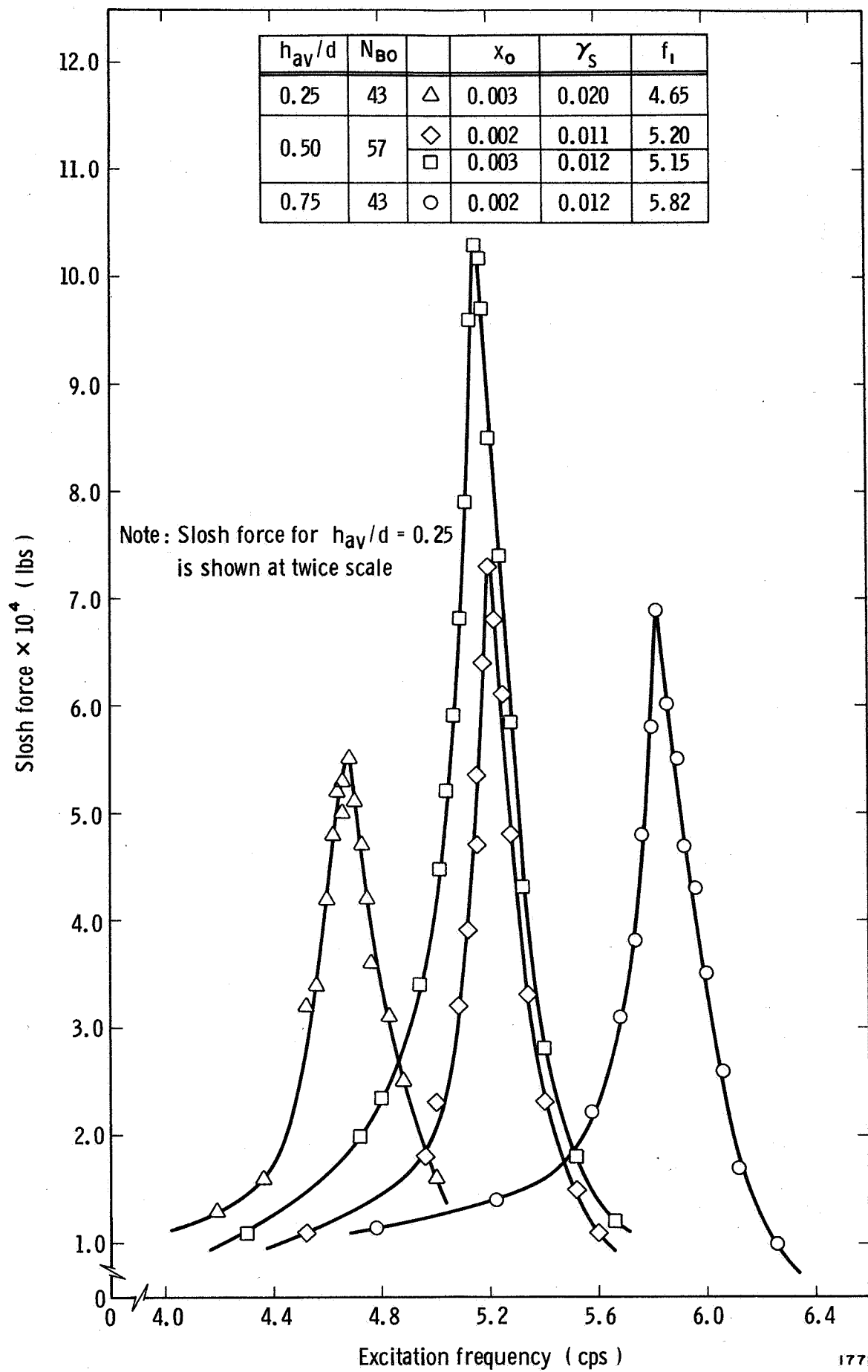


Figure 16. Force Response Curve For Acetone In 1.04" Spherical Tank

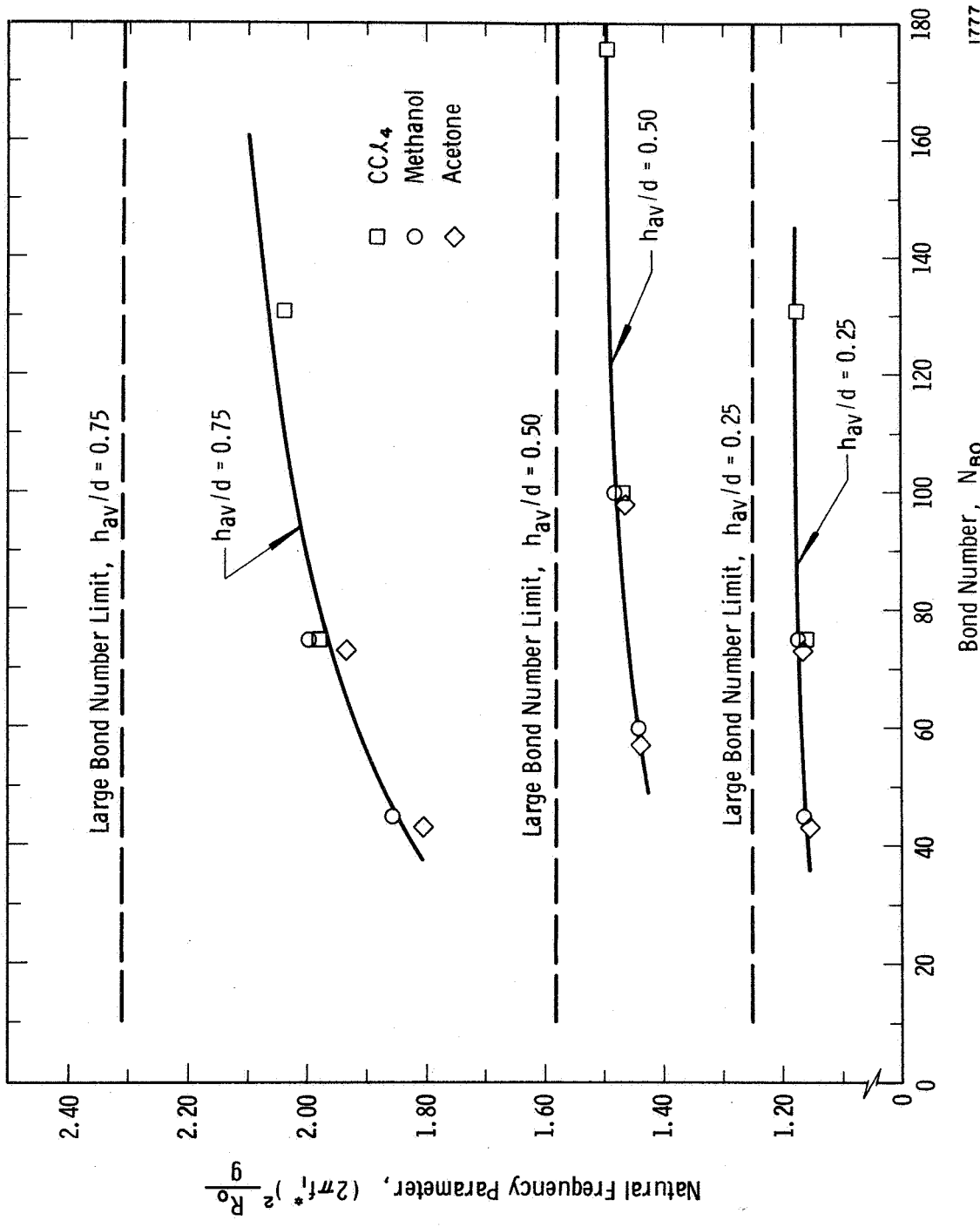


Figure 17. Variation Of Natural Frequency Parameter In Spherical Tanks With Bond Number